Colloids and Surfaces B: Biointerfaces 167 (2018) 425–431

Contents lists available at ScienceDirect

Colloids and Surfaces B: Biointerfaces

journal homepage: www.elsevier.com/locate/colsurfb

Magnetic nanoparticle decorated graphene based electrochemical nanobiosensor for H_2O_2 sensing using HRP

P.P. Waifalkar[a], A.D. Chougale[b], P. Kollu[c,d], P.S. Patil[a], P.B. Patil[e,*]

[a] Thin Film Materials Laboratory, Department of Physics, Shivaji University, Kolhapur, MS, India
[b] Department of Chemistry, The New College, Shivaji University, Kolhapur, MS, India
[c] Department of Metallurgical Engineering and Materials Science, Indian Institute of Technology Bombay, Mumbai, MS, India
[d] Thin Film Magnetism group, Cavendish Laboratory, Department of Physics, University of Cambridge, Cambridge CB3 0HE, UK
[e] Department of Physics, The New College, Shivaji University, Kolhapur, MS, India

ARTICLE INFO

Article history:
Received 6 September 2017
Received in revised form 19 April 2018
Accepted 21 April 2018
Available online 22 April 2018

Keyword:
Magnetic nanoparticle decorated graphene
MNP
RGO
H_2O_2
Horseradish peroxidase
Electrochemical biosensor

ABSTRACT

To utilize synergetic effect of graphene's higher conductivity and magnetic nanoparticles biocompatibility, an electrochemical nanobiosensor is constructed based on magnetic nanoparticle decorated graphene (MRGO) using Horseradish peroxidase (HRP) for H_2O_2 sensing. Sensors based on magnetic nanoparticles (MNP) and reduced graphene oxide (RGO) are studied for comparison. MNP, RGO and MRGO were characterized by X-ray diffraction (XRD), Transmission electron microscopy (TEM) and Fourier transform infrared spectroscopy (FTIR). XRD studies have confirmed successful synthesis of Fe_3O_4 MNPs, RGO and MRGO. TEM micrographs revealed uniform decoration of MNPs on graphene. FTIR confirmed the immobilization of HRP on MNP, RGO and MRGO. The MRGO based sensor exhibited higher sensitivity (48.08 μA μM^{-1} cm^{-2}) compared to MNP (39.08 μA μM^{-1} cm^{-2}) and RGO (41.08 μA μM^{-1} cm^{-2}) based biosensors.

1. Introduction

Hydrogen peroxide (H_2O_2) sensing is very important in many areas like food industry, pharmaceutical industry, clinical diagnosis and also in environmental investigates. Being an indicator of oxidative stress H_2O_2 is the trademark of many disorders including atherosclerosis, alzheimer's and cancer. Numerous oxidases through different biological reactions are responsible to increase the H_2O_2 content in the body [1,2] and therefore the determination of H_2O_2 is essential in many clinical diagnoses. Many techniques have been developed to detect H_2O_2, including titrimetry [3], fluorimetry [4], spectrophotometry [5], chemiluminescence [6] and electrochemical sensors [7–10]. Many of them are high cost and time consuming, except for electrochemical sensors. Due to its simplicity, high sensitivity and selectivity electrochemical methods are extensively investigated for H_2O_2 determination. Enzymes are well known for their specificity, sensitivity and fast activity towards their substrates. Horseradish peroxidase (HRP) catalyses the reaction where H_2O_2 gets converted to H_2O and oxygen radical which can be measured by electrochemical methods. Along with this HRP is easily available in high purity and low cost and hence is most extensively studied in the development biosensors [11–24].

It is well understood that the modification of electrode materials play a significant role in performance of electrochemical sensor for detecting target molecules. Magnetic nanoparticles (MNPs) with their unique properties like high surface energy, large surface area and functioning as electron-conducting pathways facilitates electron transfer between redox systems and bulk-electrode materials [25,26]. MNPs may also establish interfaces for the electrocatalysis of redox processes of molecules (e.g., H_2O_2, O_2 or NADH) involved in many significant biochemical reactions [27]. The handling time for sample pre-treatment can be minimised by using magnetic properties of MNPs which eliminate the need of centrifugation or chromatography [28]. Most iron oxide MNPs are biocompatible and they can be functionalized or encapsulated in polymers, metal or silica NPs, or carbon materials to increase the functionalities [29]. Thus, iron oxide based MNPs provide a promising experimental platform for developing electrochemical biosensor. A high-performance biosensor has been reported from chitosan/Fe_3O_4 nanocomposites [30]. Due to its high specific surface area, exceptional electrical conductivity and biocompatibility, graphene could be the excellent material to modify electrode [31–33]. Considering these facts, the combination of magnetic nanoparticles and graphene can be a promising material to mod-

* Corresponding author.
E-mail address: prashantphy@gmail.com (P.B. Patil).

https://doi.org/10.1016/j.colsurfb.2018.04.042
0927-7765/

ify electrode for obtaining improved performance of biosensor. In previous reports reduced graphene oxide (rGO)/Fe_3O_4 nanocomposite has also been utilized for the sensing of H_2O_2 [34]. The Fe_3O_4/rGO modified electrode employed for sensing ascorbic acid (AA) and other substances, applying the combined effect of magnetic nanoparticles and graphene report, showed higher sensitivity with a wide linear range [35–37]. Chitosan is the natural polymer, which has been considered as the most promising substrate for enzyme immobilization due to its biocompatibility and multiple functional groups [33,38,39].

In this work, magnetic particle decorated graphene (MRGO) is synthesized to combine magnetic nanoparticle's catalytic activity and larger active surface area along with superior conductivity of graphene. Here we have evaluated and compared performance of electrochemical biosensors constructed by immobilizing HRP on the chitosan coated MNPs, RGO and MRGO for the detection of H_2O_2.

2. Materials and methods

Graphite powder and HRP was procured from Sigma Aldrich, India. Ferric chloride ($FeCl_3{\cdot}6H_2O$), ferrous chloride ($FeCl_2{\cdot}4H_2O$), NH_3, hydrazine hydrate and sodium nitrite were procured from Sd fine Chemicals India. Phosphate buffer solution (PBS) solution (0.1 M) was prepared with sodium dihydrogen phosphate (NaH_2PO_4) and disodium hydrogen phosphate (Na_2HPO_4) and used as supporting electrolyte throughout electrochemical studies. The chemicals used for PBS solution were purchased from Himedia, India. All chemicals mentioned here were of analytical reagent grade and were used as received. Double distilled water was used for all the experiments.

2.1. Preparation of MNPs, RGO and MRGO

The details of experiments are given in Supporting Information. The Fe_3O_4 magnetic nanoparticles were prepared by co-precipitation method. Graphite powder was oxidized to graphene oxide (GO) by Hummer's method [40]. The GO was dispersed in 450 ml double distilled water and reduced with 1 ml of hydrazine hydrate at 90 °C for 4 h, to produce reduced graphene oxide (RGO) nanosheets.

The MNP decorated reduced graphene oxide (MRGO) was synthesized by method reported by Chandra et al., 2010, in which simultaneous reduction of GO and coprecipitation of iron salts has been carried out [41]. Briefly, 0.7 g GO was first dispersed in 450 ml distilled water. Ferric chloride (3.24 g) and ferrous chloride (1.26 g) were separately dissolved in 25 ml distilled water and mixed with 2:1 molar ratio. The prepared solution of ferric and ferrous ions was slowly added to GO solution at room temperature. Then the pH of solution was adjusted to 10 by using 30% ammonia solution. The strong reducing agent, hydrazine hydrate (10 ml) was added with constant stirring at 90 °C. The resulting black colour solution was stirred vigorously for 4 h and the solution was cooled to room temperature. The black MRGO nanocomposite obtained was magnetically separated from solution. MRGO was then washed several times with water and ethanol and finally dried in a vacuum.

2.2. HRP complex preparation

The 10 mg/ml suspension of MNPs in water was prepared. Chitosan coated MNPs were prepared by stirring MNPs suspension and acylated chitosan in equal proportion for 3 h. Chitosan coated MNPs were then obtained by washing it 2 times by magnetic decantation with double distilled water. HRP and chitosan coated MNPs in equal proportion were gently shaken and incubated for 2 h at room temperature to immobilize HRP on chitosan coated MNPs.

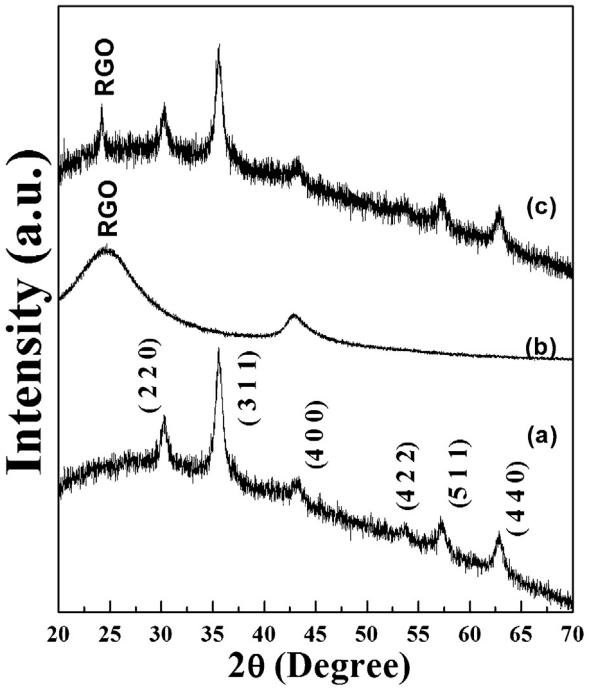

Fig. 1. XRD patterns of a) MNPs, b) RGO and c) MRGO.

HRP immobilized MNPs are denoted as MNP/chit/HRP. Other electrode modifying materials, viz. RGO/chit/HRP and MRGO/chit/HRP are prepared by similar protocols.

2.3. Preparation of modified electrodes

Prior to modification, platinum electrode was carefully polished with 0.3 μm alumina powder and rinsed thoroughly with pure water. After polishing, sonicated in ethanol and pure water for 5 min respectively and dried with nitrogen. The 10 μl of the HRP complex was casted onto the surface of the platinum electrode. Prepared electrode was dried in vacuum at room temperature. For comparison, Pt/MNP/chit/HRP, Pt/RGO/chit/HRP and Pt/MRGO/chit/HRP electrodes were modified with similar method.

3. Results and discussion

Powder X-ray diffraction (XRD) patterns were obtained and analysed for MNPs, RGO and MRGO composites (Fig. 1). As can be seen, the patterns of MNP (Fig. 1(a)) and MRGO (Fig. 1(c)) exhibited diffraction peaks corresponding to Fe_3O_4. The peak positions and relative intensities match well with the standard XRD data for Fe_3O_4 (JCPDS file No. 75-0033). The broad peak around 23.9^0 in XRD pattern of RGO shown in Fig. 1(b) corresponds to RGO. This RGO peak also exists in MRGO pattern, which confirms successful synthesis of MNP decorated RGO.

Fourier Transform Infrared Spectroscopy (FTIR) was used for characterisation of the MNP/chit/HRP, RGO/chit/HRP and MRGO/chit/HRP composites before casting on the Pt electrode (Fig. 2). The presence of magnetite nanoparticles can be seen by strong absorption bands at around 602 cm^{-1}. Previously, the characteristic absorption bands of the Fe – O was reported at the 590 cm^{-1} [39]. However due to finite size effect of nanoparticles, the breaking of a large number of bonds for surface atoms has resulted in the rearrangement of un-localized electrons on the particle surface [42]. The absorption band at 1632 cm^{-1} attributed to C=O of acetylated (-$CONH_2$) group confirms the chitosan existence in all three composites. Peaks at 1550 cm^{-1} can be understood

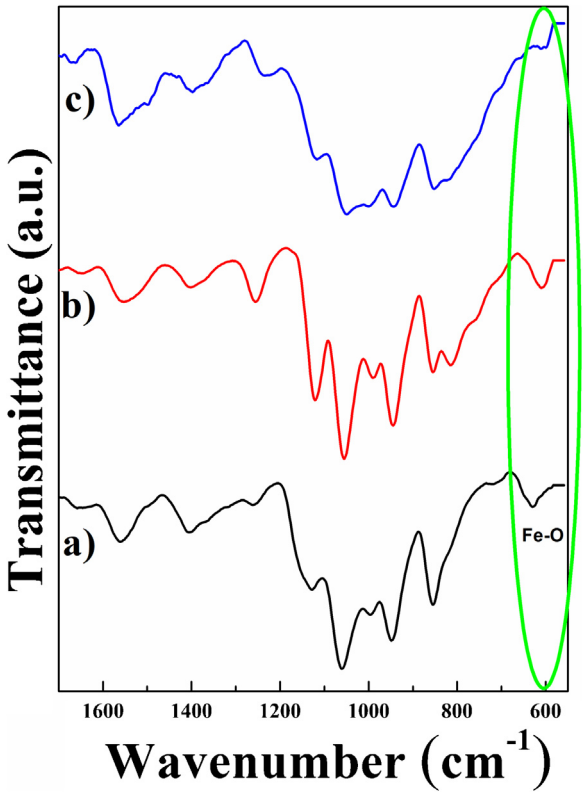

Fig. 2. FTIR spectra of a) MNP/chit/HRP, b) RGO/chit/HRP and c) MRGO/chit/HRP.

to arise from amide I linkages of HRP molecules [43]. The peak of 1548 cm^{-1} found in the RGO and MRGO containing complexes which is due to the skeletal vibration of RGO [44].

TEM was used to reveal the microstructure of the magnetic nanoparticle decorated graphene. The low and high magnification TEM images of MRGO are shown in Fig. 3(a) and (b). Presence of RGO and Fe_3O_4 nanoparticles can be clearly observed and it is evident that two dimensional RGO sheets are uniformely decorated by a large quantity of Fe_3O_4 nanostructures.

3.1. Electrochemical properties of the biosensor

Cyclic voltammetry was used to study the electroanalytical properties of the fabricated hydrogen peroxide biosensor.

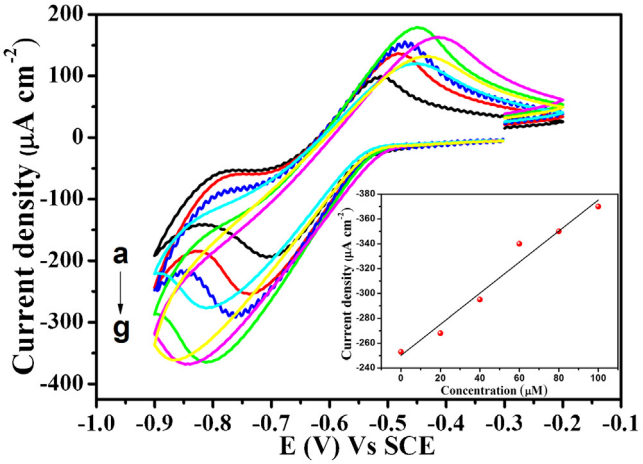

Fig. 4. CVs of Pt/MNP/chit/HRP electrode in 0.1 mol/L PBS (pH 7) with various concentrations of H_2O_2 (a–g) Bare, 00, 20, 40, 60, 80, 100 μM at 100 mV/s scan rate. Inset: The calibration plot of Pt/MNP/chit/HRP electrode (scan rate: 100 mV/s).

Fig. 4 shows the cyclic voltammograms of Pt/MNP/chit/HRP in 0.1 mol/L deaerated PBS (pH 7) for different concentrations of H_2O_2 (0–100 μM) for potential range of −0.2 to −0.9 V at scan rate 100 mV/s. It can be seen from Fig. 4 that when the H_2O_2 exists, the reduction peak current is increased compared to that for bare Pt electrode. This shows that the reduction of H_2O_2 was appeared on the surface of the electrode. Further it can be seen that with increasing concentration of H_2O_2 the reduction peak current increases rapidly. Here HRP gets converted to oxidized form due to H_2O_2, which is then reduced at the electrode surface by direct transfer of electron. Therefore, the reductive current increases linearly with H_2O_2 concentration. The calibration plot of Pt/MNP/chit/HRP biosensor towards H_2O_2 is extracted from cyclic voltammograms and is depicted in inset of Fig. 4. It is evident from this figure that the calibration plot of the biosensor is in a linear relationship with the concentration of H_2O_2 and the sensitivity is 39.80 μA μM^{-1} cm^{-2}. Many studies has been undertaken to evaluate the sensitivity of the Fe_3O_4 magnetic particles based electrodes. Yuan et al. have found the linear response range of the sensor from 10.0×10^{-6} to 140.0×10^{-6} M and a sensitivity was 11.05 μA mM^{-1} for hydrothermally synthesized Fe_3O_4 magnetic particles [45]. Cao et al. reported H_2O_2 electrochemical sensor based on Fe_3O_4 nanoparticles and sensitivity of the sensor was 0.77683 μA mM^{-1} and the detection limit was estimated to be about 1 mM [46]. Qu et al. have reported

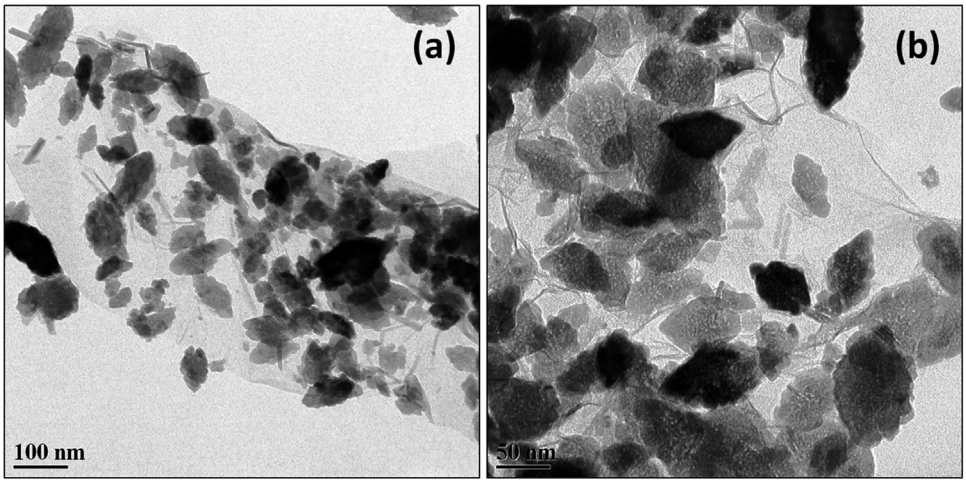

Fig. 3. TEM of MRGO.

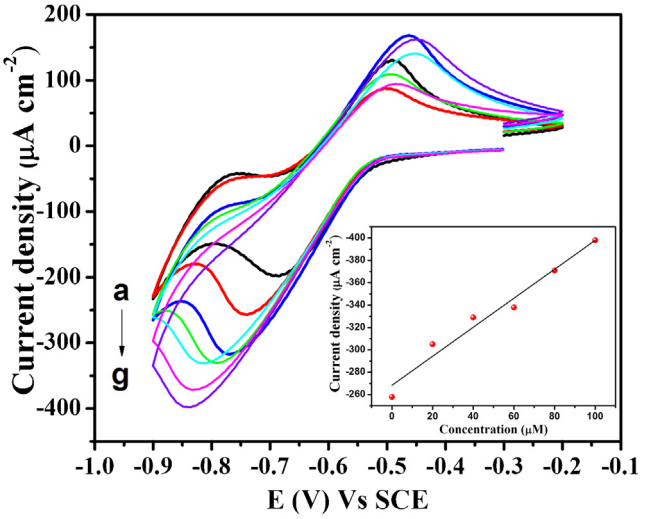

Fig. 5. CVs of Pt/RGO/chit/HRP electrode in 0.1 mol/L PBS (pH 7) with various concentrations of H_2O_2 (a–g) Bare, 00, 20, 40, 60, 80, 100 μM at 100 mV/s scan rate. Inset: The calibration plot of Pt/RGO/chit/HRP electrode (scan rate: 100 mV/s).

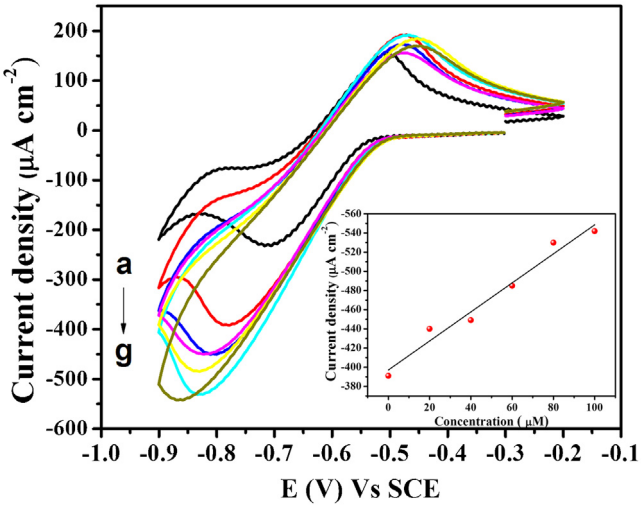

Fig. 6. CVs of Pt/MRGO/chit/HRP electrode in 0.1 mol/L PBS (pH 7) with various concentrations of H_2O_2 (a–g) Bare, 00, 20, 40, 60, 80, 100 μM at 100 mV/s scan rate. Inset: The calibration plot of Pt/MRGO/chit/HRP electrode (scan rate: 100 mV/s).

the electrochemical behavior of hydrogen peroxide sensor by cyclic voltammetry where Fe_3O_4 magnetic nanoparticles were synthesized by chemical co-precipitation with sodium citrate surfactant. They found the peak current increased linearly with concentration from 1.00×10^{-5} to 1.00×10^{-3} mol/L with a detection limit of 1.53×10^{-6} mol/L [47].

The cyclic voltammetry has also been obtained for RGO modified electrode for H_2O_2 sensing. Fig. 5 shows the cyclic voltammograms of Pt/RGO/chit/HRP in 0.1 mol/L deaerated PBS (pH 7) for 0–100 μM concentrations of H_2O_2 in potential range of −0.2 to −0.9 V at scan rate 100 mV/s. The linear increment in reduction current was observed with increasing concentration of H_2O_2 as evident from calibration plot (inset of Fig. 5). The high conductivity of RGO provides more conduction pathways for the electron-transfer which has led to the increased peak current [48,35]. Hence, for Pt/RGO/chit/HRP electrode the enhancement of reduction peak current along with linearity with increasing concentration of H_2O_2 was observed as compared to Pt/MNP/chit/HRP electrode. The sensitivity of RGO modified electrode is 41.08 μA μM^{-1} cm^{-2} which is higher than that of MNP modified electrode. Along with higher conductivity, the large electroactive surface area of RGO is responsible for the improvement in sensitivity. Previously HRP functionalized graphene has been utilised for H_2O_2 amperometric sensor showed a fast response of < 2 s at 0.02 V [49,50]. In another report H_2O_2 biosensor has been constructed, based on the HRP entrapped onto the as prepared graphene/PANI, which showed an sensitivity of 294.9 μA mM^{-1} for the detection of H_2O_2 [51].

To evaluate combined effect of MNPs and RGO on the signal transduction, Pt/MRGO/chit/HRP electrode was studied by cyclic voltammetry. The cyclic voltammograms of this modified electrode in 0.1 mol/L deaerated PBS (pH 7.0) at 100 mV/s potential scan rate was recorded for different concentrations of H_2O_2 (0–100 μM) for potential window of −0.2 to −0.9 V (Fig. 6). The cyclic voltammetry of Pt/MRGO/chit/HRP modified electrode shows the higher reduction peak current values with addition of H_2O_2 than that of Pt/MNP/chit/HRP and Pt/RGO/chit/HRP electrodes. The peak reduction currents of the Pt/MRGO/chit/HRP electrode increased significantly for each addition of H_2O_2. The electron transfer rate increased significantly due to RGO sheets whereas MNPs decorated on RGO facilitated the catalytic sites of HRP accessible to H_2O_2 [48]. The enhanced linear response of Pt/MRGO/chit/HRP electrode biosensor with concentration of H_2O_2 is revealed in the calibration plot shown in inset of Fig. 6. The sensitivity of MRGO modified electrode is 48.08 μA μM^{-1} cm^{-2} which is higher than MNP or RGO modified electrodes. Earlier reported MRGO based electrodes have also showed improved sensitivity. Xiong et al. have developed a non-enzymatic hydrogen peroxide (H_2O_2) sensor based on Fe_3O_4/reduced graphene oxide (Fe_3O_4/RGO) nanocomposite material. They have found sensitivity of Fe_3O_4/RGO modified electrode is higher than that of MNP and GO modified electrodes [52]. Noorbakhsh et al. have reported MRGO-chitosan modified with DNA-celestine blue and used it for determination of H_2O_2 in human serum samples. They have obtained sensitivity of 8.5 μA/μM for H_2O_2 with linear range of 0.1 −1.1 and 17–38 (μM) [53]. Yang et al. have reported electrochemical detection of H_2O_2 based on Fe_3O_4 nanoparticles decorated graphene oxide modified with polyamidoamine dendrimer. They have observed linear calibration range of 20–1000 μM with the detection limit of 2.0×10^{-6} M [54].

The apparent Michaelis – Menten constant (K_m) has been evaluated from the electrochemical version of the Lineweaver–Burk equation [55], $1/I_{ss} = (1/I_{max}) + (K_m/I_{max}.C)$, where I_{ss} is the steady state current, I_{max} is maximum current measured under saturated condition and C is the concentration. The K_m value of the MRGO biosensor was found to be 0.19 mM, which is lower than the reported values [56–58]. Further, we studied the relationship between redox peak potentials and scan rate to investigate the electron transfer kinetics using the Laviron equation (1) [59].

$$\log k_s = \alpha \log(1-\alpha) + (1-\alpha)log - \log\left(\frac{RT}{nF\nu}\right)\frac{\alpha(1-\alpha)nF\left(\Delta E_p\right)}{2.3RT} \quad (1)$$

Where, R is the universal gas constant (8.314 J mol^{-1} K^{-1}), T is the room temperature (298.5 K) and ΔEp is the peak separation and F is faraday's constant. The number of electrons transferred is considered as 1 and α value is assumed as ≈ 0.5. The electron transfer rate constant (k_s) of HRP in this study was calculated to be 1.43 s^{-1}. This value is comparable with previously published studies [60,61]. The electrochemical impedance spectroscopy (EIS) was employed to study the electron transfer properties at the surface of the electrode. Fig. 8 shows the Nyquist plots of the impedance spectroscopy of the bare Pt and Pt/MRGO/chit/HRP electrodes in the frequency range of 50–5 × 10^5 Hz. The electron transfer resistance (R_{et}) at the surface of the electrode is equal to the semi-circle diameter. The diame-

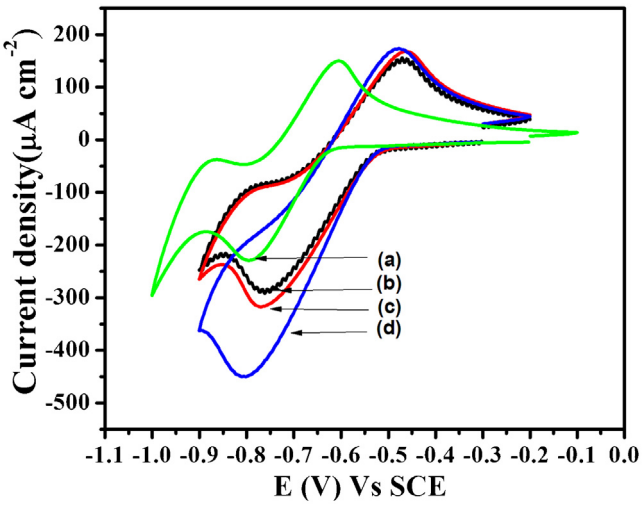

Fig. 7. CVs of a) Pt/MNP/chit/HRP, b) Pt/RGO/chit/HRP and c) Pt/MRGO/chit/HRP electrodes in 0.1 mol/L PBS (pH 7) with 20 μM concentration of H_2O_2 at 100 mV/s.

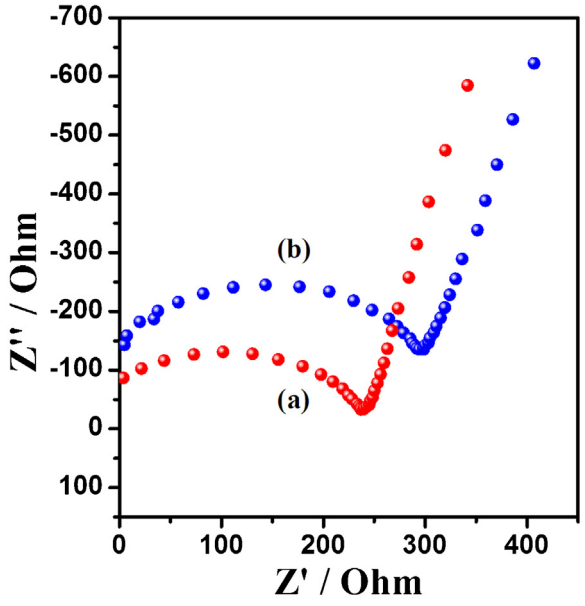

Fig. 8. EIS curves of (a) Bare Pt and (b) Pt/MRGO/chit/HRP electrodes in 5.0 mM $[Fe(CN)]^{3-/4-}$ in 0.1 M PBS solution.

ter of the semicircle for Pt/MRGO/chit/HRP electrode (curve b) is slightly larger than that of bare Pt electrode (curve a), suggesting the successful modification of the electrode.

In order to explain the differentiated response of all the three modified electrodes, the cyclic voltammograms of these electrodes along with the bare electrode are plotted in Fig. 7 for similar concentration of H_2O_2 (20 μM). The cyclic voltammograms of bare Pt was obtained between −0.1 and −1.0 V. Self-catalyzing capacity of platinum towards H_2O_2 reduction is responsible for the small reduction current with bare platinum electrode. Also bare electrodes response to H_2O_2 is not linear which is obvious because of its limited catalytic activity (supplementary information) [62]. As can be seen in Fig. 7 response current of MNP, RGO and MRGO modified electrodes are in increasing order respectively. Every carbon atom of RGO sheets is exposed on its surfaces, so minute changes in the charge in its vicinity can give measurable transduction signal [49]. This characteristic of RGO provides a favorable microenvironment for HRP and promotes the direct electron transfer from oxidized HRP to electrode which results in better response of RGO

Table 1
The recovery of the real sample analysis at the Pt/MRGO/chit/HRP modified electrode.

Sample	H_2O_2 added (μM)	H_2O_2 measured (μM)	Recovery (%)
1	60	59.68	99.46
2	80	79.37	99.21
3	100	98.83	98.83

modified electrode compare to MNP modified electrode. In case of MRGO modified electrode, along with better charge transfer capacity and high surface area of RGO, MNPs provides better stability to enzyme. This synergetic effect of RGO and MNPs results in better performance of MRGO modified electrode (Pt/MRGO/chit/HRP).

3.2. Real sample analysis

To test the practicability, the MRGO modified electrode was used to determine H_2O_2 in natural orange juice. The 10 ml orange juice sample was diluted down to 40 ml with a 0.1 M PBS (pH 7.0). Then, known amounts of H_2O_2 were added and their recoveries were determined using developed sensor. The results are listed in Table 1 and it can be seen that the measured H_2O_2 concentrations are close to that of added amount of H_2O_2. This suggests that the matrix of orange juice sample does not interfere the H_2O_2 sensing of developed sensor.

4. Conclusions

Fe_3O_4 magnetic nanoparticles, RGO and MNP decorated graphene were successfully synthesized. In MRGO, MNPs are uniformly decorated over RGO. Synthesized MNP, RGO and MRGO were used to construct modified electrodes which have shown the linearity towards H_2O_2 sensing. Pt/MRGO/chit/HRP has shown improved sensitivity (48.08 μA μM^{-1} cm^{-2}) compared to Pt/MNP/chit/HRP (39.80 μA μM^{-1} cm^{-2}) and Pt/RGO/chit/HRP (41.08 μA μM^{-1} cm^{-2}). MRGO modified electrode presented better sensing than that of MNP and RGO modified electrodes. MNP provides the better stability to HRP, whereas RGO offers better conductivity and larger surface area for HRP immobilization. The synergy of these two has been utilized so that the MRGO modified electrode exhibits improved electrochemical response compared to MNP and RGO modified electrodes.

Conflicts of interest

None.

Acknowledgment

The authors acknowledges DST, New Delhi for funding through DST-EMR project EMR/2017/001810.

Appendix A. Supplementary data

Supplementary data associated with this article can be found, in the online version, at https://doi.org/10.1016/j.colsurfb.2018.04.042.

References

[1] A.A. Karyakin, O.V. Gitelmacher, E.E. Karyakina, Prussian blue-based first-generation biosensor. A sensitive amperometric electrode for glucose, Anal. Chem. 67 (1995) 2419–2423, http://dx.doi.org/10.1021/ac00110a016.
[2] L. Wang, E. Wang, A novel hydrogen peroxide sensor based on horseradish peroxidase immobilized on colloidal Au modified ITO electrode, 2003, http://dx.doi.org/10.1016/j.elecom.2003.12.004.

[3] N.V. Kiassen, D. Marchington, H.C.E. Mcgowant, H_2O_2 determination by the I3- method and by KMnO4 titration, Anal. Chem. 66 (1994) 2921–2925, http://dx.doi.org/10.1021/ac00090a020.
[4] M.C.Y. Chang, A. Pralle, E.Y. Isacoff, C.J. Chang, A selective, cell-permeable optical probe for hydrogen peroxide in living cells, J. Am. Chem. Soc. 126 (2004) 15392–15393, http://dx.doi.org/10.1021/ja0441716.
[5] C. Matsubara, N. Kawamoto, K. Takamura, Oxo[5,10, 15, 20-tetra(4-pyridyl)porphyrinato]titanium(IV): an ultra-high sensitivity spectrophotometric reagent for hydrogen peroxide, Analyst 117 (1992) 1781, http://dx.doi.org/10.1039/an9921701781.
[6] D.W. King, W.J. Cooper, S.A. Rusak, B.M. Peake, J.J. Kiddle, D.W. O'Sullivan, M.L. Melamed, C.R. Morgan, S.M. Theberge, Flow injection analysis of H_2O_2 in natural waters using acridinium ester chemiluminescence: method development and optimization using a kinetic model, Anal. Chem. 79 (2007) 4169–4176, http://dx.doi.org/10.1021/ac062228w.
[7] Y.X. Chen, K.J. Huang, L.L. He, Y.H. Wang, Tetrahedral DNA probe coupling with hybridization chain reaction for competitive thrombin aptasensor, Biosens. Bioelectron. 100 (2018) 274–281, http://dx.doi.org/10.1016/j.bios.2017.09.022.
[8] Y.X. Chen, K.J. Huang, K.X. Niu, Recent advances in signal amplification strategy based on oligonucleotide and nanomaterials for microRNA detection-a review, Biosens. Bioelectron. 99 (2018) 612–624, http://dx.doi.org/10.1016/j.bios.2017.08.036.
[9] H.L. Shuai, X. Wu, K.J. Huang, Z.B. Zhai, Ultrasensitive electrochemical biosensing platform based on spherical silicon dioxide/molybdenum selenide nanohybrids and triggered Hybridization Chain Reaction, Biosens. Bioelectron. 94 (2017) 616–625, http://dx.doi.org/10.1016/j.bios.2017.03.058.
[10] Y.H. Wang, K.J. Huang, X. Wu, Recent advances in transition-metal dichalcogenides based electrochemical biosensors: a review, Biosens. Bioelectron. 97 (2017) 305–316, http://dx.doi.org/10.1016/j.bios.2017.06.011.
[11] L. Qian, X. Yang, Composite film of carbon nanotubes and chitosan for preparation of amperometric hydrogen peroxide biosensor, Talanta 68 (2006) 721–727, http://dx.doi.org/10.1016/j.talanta.2005.05.030.
[12] J.-L. Huang, Y.-C. Tsai, Direct electrochemistry and biosensing of hydrogen peroxide of horseradish peroxidase immobilized at multiwalled carbon nanotube/alumina-coated silica nanocomposite modified glassy carbon electrode, Sens. Actuators B Chem. 140 (2009) 267–272, http://dx.doi.org/10.1016/j.snb.2009.04.033.
[13] S. Cao, R. Yuan, Y. Chai, L. Zhang, X. Li, F. Gao, A mediator-free amperometric hydrogen peroxide biosensor based on HRP immobilized on a nano-Au/poly 2, 6-pyridinediamine-coated electrode, Bioprocess Biosyst. Eng. 30 (2007) 71–78, http://dx.doi.org/10.1007/s00449-006-0100-1.
[14] S. Chen, R. Yuan, Y. Chai, B. Yin, W. Li, L. Min, Amperometric hydrogen peroxide biosensor based on the immobilization of horseradish peroxidase on core-shell organosilica@chitosan nanospheres and multiwall carbon nanotubes composite, Electrochim. Acta 54 (2009) 3039–3046, http://dx.doi.org/10.1016/j.electacta.2008.12.009.
[15] X. Liu, L. Luo, Y. Ding, Y. Xu, F. Li, Hydrogen peroxide biosensor based on the immobilization of horseradish peroxidase on γ-Al2O3 nanoparticles/chitosan film-modified electrode, J. Solid State Electrochem. 15 (2011) 447–453, http://dx.doi.org/10.1007/s10008-010-1120-y.
[16] A.S. Ahammad, Hydrogen peroxide biosensors based on horseradish peroxidase and hemoglobin, J. Biosens. Bioelectron. 9 (2013) 1–11, http://dx.doi.org/10.4172/2155-6210.S9-001.
[17] F. Chekin, L. Gorton, I. Tapsobea, Direct and mediated electrochemistry of peroxidase and its electrocatalysis on a variety of screen-printed carbon electrodes: amperometric hydrogen peroxide and phenols biosensor, Anal. Bioanal. Chem. 407 (2015) 439–446, http://dx.doi.org/10.1007/s00216-014-8282-x.
[18] F. Kazenwadel, H. Wagner, B.E. Rapp, M. Franzreb, Optimization of enzyme immobilization on magnetic microparticles using 1-ethyl-3-(3-dimethylaminopropyl)carbodiimide (EDC) as a crosslinking agent, Anal. Methods 7 (2015) 10291–10298, http://dx.doi.org/10.1039/C5AY02670A.
[19] T.M. Freire, L.M.U. Dutra, D.C. Queiroz, Ricardo N.M.P.S, K. Barreto, J.C. Denardin, F.R. Wurm, C.P. Sousa, A.N. Correia, P. De Lima-Neto, P.B.A. Fechine, Fast ultrasound assisted synthesis of chitosan-based magnetite nanocomposites as a modified electrode sensor, Carbohydr. Polym. 151 (2016) 760–769, http://dx.doi.org/10.1016/j.carbpol.2016.05.095.
[20] D. Lu, F. Lu, G. Pang, A novel tetrahydrocannabinol electrochemical nano immunosensor based on horseradish peroxidase and Double-Layer gold nanoparticles, Molecules 21 (2016), http://dx.doi.org/10.3390/molecules21101377.
[21] D. Sović, A. Gajović, D. Iveković, Bioelectrocatalytic and biosensing properties of horseradish peroxidase covalently immobilized on (3-aminopropyl)trimethoxysilane-modified titanate nanotubes, Electrochim. Acta 56 (2011) 9953–9960, http://dx.doi.org/10.1016/j.electacta.2011.08.077.
[22] X. Bin Kang, G.C. Pang, X.Y. Liang, M. Wang, J. Liu, W.M. Zhu, Study on a hydrogen peroxide biosensor based on horseradish peroxidase/GNPs-thionine/chitosan, Electrochim. Acta 62 (2012) 327–334, http://dx.doi.org/10.1016/j.electacta.2011.12.034.
[23] A. Muthurasu, V. Ganesh, Horseradish peroxidase enzyme immobilized graphene quantum dots as electrochemical biosensors, Appl. Biochem. Biotechnol. 174 (2014) 945–959, http://dx.doi.org/10.1007/s12010-014-1019-7.
[24] R. Zhang, W. Chen, Recent advances in graphene-based nanomaterials for fabricating electrochemical hydrogen peroxide sensors, Biosens. Bioelectron. 89 (2017) 249–268, http://dx.doi.org/10.1016/j.bios.2016.01.080.
[25] M. Hasanzadeh, N. Shadjou, M. de la Guardia, Iron and iron-oxide magnetic nanoparticles as signal-amplification elements in electrochemical biosensing, TrAC Trends Anal. Chem. 72 (2015) 1–9, http://dx.doi.org/10.1016/j.trac.2015.03.016.
[26] D. Grieshaber, R. Mackenzie, J. Vörös, E. Reimhult, Electrochemical biosensors -sensor principles and architectures, Sensors 8 (2008) 1400–1458, http://dx.doi.org/10.3390/s8031400.
[27] H. Wei, E. Wang, Electrochemiluminescence of tris(2, 2′-bipyridyl)ruthenium and its applications in bioanalysis: a review, Luminescence 26 (2011) 77–85, http://dx.doi.org/10.1002/bio.1279.
[28] S. Mahiuddin, A. Renoncourt, P. Bauduin, D. Touraud, W. Kunz, Horseradish peroxidase activity in a reverse catanionic microemulsion, Langmuir 21 (2005) 5259–5262, http://dx.doi.org/10.1021/la047161r.
[29] B. Paczosa-Bator, J. Migdalski, A. Lewenstam, Conducting polymer films as model biological membranes: electrochemical and ion-exchange properties of poly(pyrrole) films doped with asparagine and glutamine, Electrochim. Acta (2006) 2173–2181, http://dx.doi.org/10.1016/j.electacta.2005.03.084.
[30] A. Kaushik, R. Khan, P.R. Solanki, P. Pandey, J. Alam, S. Ahmad, B. Malhotra, Iron oxide nanoparticles–chitosan composite based glucose biosensor, Biosens. Bioelectron. 24 (2008) 676–683, http://dx.doi.org/10.1016/j.bios.2008.06.032.
[31] S. Alwarappan, A. Erdem, C. Liu, C.-Z. Li, Probing the Electrochemical Properties of Graphene Nanosheets for Biosensing Applications, (n.d.). 10.1021/jp9010313.
[32] X. Kang, J. Wang, I.A. Wu, J. Liu, Y. Lin, Glucose oxidase–graphene–chitosan modified electrode for direct electrochemistry and glucose sensing, Biosens. Bioelectron. 25 (2009) 901–905, http://dx.doi.org/10.1016/j.bios.2009.09.004.
[33] Y.X. Chen, K.J. Huang, F. Lin, L.X. Fang, Ultrasensitive electrochemical sensing platform based on graphene wrapping SnO_2 nanocorals and autonomous cascade DNA duplication strategy, Talanta 175 (2017) 168–176, http://dx.doi.org/10.1016/j.talanta.2017.07.042.
[34] Y. Ye, T. Kong, X. Yu, Y. Wu, K. Zhang, X. Wang, Enhanced nonenzymatic hydrogen peroxide sensing with reduced graphene oxide/ferroferric oxide nanocomposites, Talanta 89 (2012) 417–421, http://dx.doi.org/10.1016/j.talanta.2011.12.054.
[35] H. Teymourian, A. Salimi, S. Khezrian, Fe_3O_4 magnetic nanoparticles/reduced graphene oxide nanosheets as a novel electrochemical and bioeletrochemical sensing platform, Biosens. Bioelectron. 49 (2013) 1–8, http://dx.doi.org/10.1016/j.bios.2013.04.034.
[36] Y. Li, X.R. Zhao, P. Li, Y.F. Huang, J. Wang, J.M. Zhang, Highly sensitive Fe_3O_4 nanobeads/graphene-based molecularly imprinted electrochemical sensor for 17 beta-estradiol in water, Anal. Chim. Acta 884 (2015) 106–113, http://dx.doi.org/10.1016/j.aca.2015.05.022.
[37] L. Yu, H. Wu, B. Wu, Magnetic Fe_3O_4 –reduced graphene oxide nano-composites-based electrochemical biosensing, Nano Micro Lett. 6 (2014) 258–267.
[38] Q. Sheng, K. Luo, L. Li, J. Zheng, Direct electrochemistry of glucose oxidase immobilized on $NdPO_4$ nanoparticles/chitosan composite film on glassy carbon electrodes and its biosensing application, Bioelectrochemistry 74 (2008) 246–253, http://dx.doi.org/10.1016/j.bioelechem.2008.08.007.
[39] P.P. Waifalkar, S.B. Parit, A.D. Chougale, S.C. Sahoo, P.S. Patil, P.B. Patil, Immobilization of invertase on chitosan coated γ-Fe_2O_3 magnetic nanoparticles to facilitate magnetic separation, J. Colloid Interface Sci. 482 (2016) 159–164, http://dx.doi.org/10.1016/j.jcis.2016.07.082.
[40] W.S. Hummers, R.E. Offeman, Preparation of graphitic oxide, J. Am. Chem. Soc. 80 (1958), http://dx.doi.org/10.1021/ja01539a017 (1339-1339).
[41] V. Chandra, J. Park, Y. Chun, J.W. Lee, I.C. Hwang, K.S. Kim, Water-dispersible magnetite-reduced graphene oxide composites for arsenic removal, ACS Nano 4 (2010) 3979–3986, http://dx.doi.org/10.1021/nn1008897.
[42] Ge Zhao, Jiu-Ju Feng, Qian-Li Zhang, Shu-Ping Li, H.-Y. Chen, Synthesis and Characterization of Prussian Blue Modified Magnetite Nanoparticles and Its Application to the Electrocatalytic Reduction of H_2O_2, 2005, http://dx.doi.org/10.1021/CM048078S.
[43] S. Singh, P.R. Solanki, M. Pandey, B. Malhotra, Covalent immobilization of cholesterol esterase and cholesterol oxidase on polyaniline films for application to cholesterol biosensor, Anal. Chim. Acta 568 (2006) 126–132, http://dx.doi.org/10.1016/j.aca.2005.10.008.
[44] R.S. Dey, C.R. Raj, Development of an amperometric cholesterol biosensor based on graphene-Pt nanoparticle hybrid material, J. Phys. Chem. C 114 (2010) 21427–21433, http://dx.doi.org/10.1021/jp105895a.
[45] K. Yuan, Y. Ni, L. Zhang, Facile hydrothermal synthesis of polyhedral Fe_3O_4 nanocrystals, influencing factors and application in the electrochemical detection of H_2O_2, J. Alloys Compd. 532 (2012) 10–15, http://dx.doi.org/10.1016/j.jallcom.2012.04.007.
[46] P. Wang, G.S. Cao, X. Li, Y. Wang, J. Li, G. Wang, Hydrogen peroxide electrochemical sensor based on Fe_3O_4 nanoparticles, Micro Nano Lett. 9 (2014) 16–18, http://dx.doi.org/10.1049/mnl.2013.0612.
[47] J. Qu, Y. Dong, T. Lou, X. Du, Determination of hydrogen peroxide using a novel sensor based on Fe_3O_4 magnetic nanoparticles, Anal. Lett. 47 (2014) 1797–1807, http://dx.doi.org/10.1080/00032719.2014.888733.
[48] J. Qu, Y. Dong, Y. Wang, T. Lou, X. Du, Determination of hydrogen peroxide using a biosensor based on Fe_3O_4 magnetic nanoparticles and horseradish peroxidase with graphene-chitosan composite, Micro Nano Lett. 9 (2014) 572–576, http://dx.doi.org/10.1049/mnl.2014.0352.

[49] S. Nandini, S. Nalini, R. Manjunatha, S. Shanmugam, J.S. Melo, G.S. Suresh, Electrochemical biosensor for the selective determination of hydrogen peroxide based on the co-deposition of palladium, horseradish peroxidase on functionalized-graphene modified graphite electrode as composite, J. Electroanal. Chem. 689 (2013) 233–242, http://dx.doi.org/10.1016/j.jelechem.2012.11.004.
[50] S. Nalini, S. Nandini, S. Shanmugam, S.E. Neelagund, J.S. Melo, G.S. Suresh, Amperometric hydrogen peroxide and cholesterol biosensors designed by using hierarchical curtailed silver flowers functionalized graphene and enzymes deposits, J. Solid State Electrochem. 18 (2014) 685–701, http://dx.doi.org/10.1007/s10008-013-2305-y.
[51] X.M. Feng, R.M. Li, Y.W. Ma, R.F. Chen, N.E. Shi, Q.L. Fan, W. Huang, One-step electrochemical synthesis of graphene/polyaniline composite film and its applications, Adv. Funct. Mater. 21 (2011) 2989–2996, http://dx.doi.org/10.1002/adfm.201100038.
[52] L.Y. Xiong, L.Z. Zheng, J.P. Xu, W. Liu, X.W. Kang, W. Wang, S.M. Yang, J. Xia, A non-enzyme hydrogen peroxide biosensor based on Fe_3O_4/RGO nanocomposite material, ECSs Electrochem Lett. 3 (2014) B26–B29, http://dx.doi.org/10.1149/2.0041412eel.
[53] A. Noorbakhsh, M. Khakpoor, M. Rafieniya, E. Sharifi, M. Mehrasa, Highly sensitive electrochemical hydrogen peroxide sensor based on iron oxide-reduced graphene oxide-chitosan modified with DNA-celestine blue, Electroanalysis 29 (2017) 1–12, http://dx.doi.org/10.1002/elan.201600660.
[54] X. Yang, L.N. Wang, G.Z. Zhou, N. Sui, Y.X. Gu, J. Wan, Electrochemical detection of H_2O_2 based on Fe_3O_4 nanoparticles with graphene oxide and polyamidoamine dendrimer, J. Clust. Sci. 26 (2015) 789–798, http://dx.doi.org/10.1007/s10876-014-0746-9.
[55] R.A. Kamin, G.S. Wilson, Rotating ring-disk enzyme electrode for biocatalysis kinetic studies and characterization of the immobilized enzyme layer, Anal. Chem. 52 (1980) 1198–1205, http://dx.doi.org/10.1021/ac50058a010.
[56] X. Kang, J. Wang, Z. Tang, H. Wu, Y. Lin, Direct electrochemistry and electrocatalysis of horseradish peroxidase immobilized in hybrid organic-inorganic film of chitosan/sol-gel/carbon nanotubes, Talanta 78 (2009) 120–125, http://dx.doi.org/10.1016/j.talanta.2008.10.063.
[57] S. Chen, R. Yuan, Y. Chai, B. Yin, W. Li, L. Min, Amperometric hydrogen peroxide biosensor based on the immobilization of horseradish peroxidase on core-shell organosilica@chitosan nanospheres and multiwall carbon nanotubes composite, Electrochim. Acta 54 (2009) 3039–3046, http://dx.doi.org/10.1016/j.electacta.2008.12.009.
[58] K. Zhou, Y. Zhu, X. Yang, C. Li, Preparation and application of mediator-free H_2O_2 biosensors of graphene-Fe_3O_4 composites, Electroanalysis 23 (2011) 862–869, http://dx.doi.org/10.1002/elan.201000629.
[59] E. Laviron, General expression of the linear potential sweep voltammogram in the case of diffusionless electrochemical systems, J. Electroanal. Chem. 101 (1979) 19–28, http://dx.doi.org/10.1016/S0022-0728(79)80075-3.
[60] S. Palanisamy, B. Unnikrishnan, S.M. Chen, An amperometric biosensor based on direct immobilization of horseradish peroxidase on electrochemically reduced graphene oxide modified screen printed carbon electrode, Int. J. Electrochem. Sci. 7 (2012) 7935–7947.
[61] X. Luo, Z. Qiu, Q. Wan, H. Shu, N. Yang, Graphene nanoplatelets and horseradish peroxidase based biosensor, Phys. Status Solidi 211 (2014) 2795–2800, http://dx.doi.org/10.1002/pssa.201431462.
[62] Y. Liu, H. Wu, M. Li, J.-J. Yin, Z. Nie, pH dependent catalytic activities of platinum nanoparticles with respect to the decomposition of hydrogen peroxide and scavenging of superoxide and singlet oxygen, Nanoscale 6 (2014) 11904–11910, http://dx.doi.org/10.1039/c4nr03848g.